Int J Clin Exp Pathol 2017;10(2):1729-1737
www.ijcep.com /ISSN:1936-2625/IJCEP0034353

Original Article

Clinicopathological characteristics and intrarenal angiotensin II expression in X-linked Alport syndrome

Xiaoqing Yang[1*], Yanjie Huang[1*], Wensheng Zhai[1], Xianqing Ren[1], Qingyin Guo[1], Xia Zhang[1], Meng Yang[1], Jian Zhang[1], Qianyi Zhao[1], Tatsuo Yamamoto[2], Yuan Sun[3], Ying Ding[1]

[1]Department of Pediatrics, The First Affiliated Hospital of Henan University of Traditional Chinese Medicine, Henan, China; [2]Division of Nephrology, Fujieda Municipal General Hospital, Shizuoka, Japan; [3]Department of Anesthesia, Stanford University School of Medicine, California, USA. [*]Equal contributors and co-first authors.

Received June 24, 2016; Accepted September 3, 2016; Epub February 1, 2017; Published February 15, 2017

Abstract: Background: The aim of this study was to assess the pathological and clinical features of children with X-linked Alport syndrome (XLAS), and to map intrarenal expression of angiotensin II (AngII). Methods: The clinical features were retrospectively analyzed in 16 children from 16 families with XLAS. Immunofluorescence for localization of α3 and α5 (type IV collagen) chains was detected. Intrarenal AngII, angiotensinogen (AGT), renin, angiotensin converting enzyme (ACE), and angiotensin II type 1 receptor (AT_1R) were examined in renal specimens by immunohistochemistry. Genetic mutations in *COL4A3, COL4A4, COL4A5* were examined in three families using exon trapping-next generation sequencing technology. Results: Hematuria was found in all 16 children with XLAS, nephrotic syndrome in 8 (males 50%, females 50%). AGT, renin, ACE and AT_1R were expressed in tubular epithelial cells, and renin also was seen in interstitium and foam cells. Compared with normal renal tissues, the intrarenal AngII expression was significantly increased in 16 children with XLAS. AngII was located in intrarenal tubules, interstitium, and foam cells and correlated with the severity of chronic tubulointerstitial lesions. Two new glycine replacement missense mutations (Gly 515 Arg and Gly 539 Val) were identified in *COL4A5* gene in two families, and one nonsense mutation of c.1117C>T (p. Arg 373 Ter) was found in *COL4A5* in one family. Conclusions: In addition to persistent proteinuria, the enhanced intrarenal AngII seems to play an important role in tubulointerstitial lesions and foam cell formation during progression of XLAS.

Keywords: Alport syndrome, clinicopathological features, intrarenal angiotensin II

Introduction

Alport syndrome (AS) is a hereditary nephropathy characterized clinically by hematuria, progressive renal insufficiency, high-tone sensorineural hearing loss, and ocular lesions [1]. AS is a relatively common genetic cause of end-stage renal disease (ESRD) in the pediatric population. The typical pathological lesion is characterized by thickening of the glomerular basement membrane (GBM) with splitting and fragmentation of the lamina densa under electron microscopy [2]. Mutations in type IV collagen genes, which cause phenotypic and functional changes in GBM and leads to AS [3]. The estimated incidence of AS is 0.729%-4.0% in renal biopsies [4, 5]. About 85% of AS are caused by X-linked mutations in *COL4A5* gene alone or both in *COL4A5* and *COL4A6* genes, which encode the α5(IV) and α6(IV) chains of type IV collagen, respectively [6]. *COL4A5* gene mutations alter GBM functions and cause progressive irregular thickening, thinning and splitting of the GBM. Nearly all affected males with X-linked AS (XLAS) develop ESRD, while heterozygous females exhibit wide variability in disease outcome [7, 8].

The more accepted and recommended treatments targeting proteinuria are via blockade of the renin-angiotensin-aldosterone system (RAAS) by angiotensin converting enzyme inhibitors (ACEI), angiotensin receptor blockers (ARB), and aldosterone inhibitors [9]. Angiotensin II (AngII) is a major effector of the RAAS. Evidence suggests the involvement of enhanced intrarenal AngII in deterioration of renal function in chronic renal disease (CKD) [10]. How-

ever, the distribution of intrarenal AngII and its relationship with other pathological injuries in XLAS remain to be clarified. The present study was designed to determine the expression of intrarenal AngII level, and the other RAAS components, including angiotensinogen (AGT), renin, angiotensin converting enzyme (ACE), angiotensin II type 1 receptor (AT_1R) in renal specimens of XLAS using immunohistochemical staining. We also analyzed in detail the clinicopathological features of XLAS using data of 16 pediatric patients. To determine the diagnosis of XLAS in three families, the exons of the *COL4A3, COL4A4, COL4A5* gene were screened for mutations by using the next-generation sequencing (NGS).

Materials and methods

Patient selection and clinical parameters

16 unrelated patients diagnosed with AS were collected at the First Affiliated Hospital of Henan University of Traditional Chinese Medicine between 2010 and 2015. The diagnostic criteria for AS applied in this study included the presence of at least three of the following five specific criteria, based on the criteria described by Flinter [11]. 1) Typical or atypical electron microscopic (EM) changes in the GBM in renal biopsy. 2) Typical or atypical collagen IV α-chain immunofluorescence (COL-IF) changes observed in renal and/or skin biopsy. 3) A family member as a proband whose diagnosis was based on EM findings and/or COL-IF in renal/skin biopsy, or on a detailed family history indicative of an X-Linked mode. 4) Definite evidence of high-tone deafness, in both ears, with or without clinical deafness. 5) Definite evidence of lens abnormality (anterior or posterior lenticonus) and/or flecks in the peripheral or mid-peripheral retinal area.

The clinical features selected for analysis included age, sex, duration from disease onset, renal clinical presentation, hematuria, serum cystatin C (CysC), creatinine clearance (Ccr, calculated by the formula: [(Urine creatinine × 24-hour urine volume)/(serum creatinine × 1440)] × [1.73 (m^2)/body surface area (m^2)]) and systolic and diastolic blood pressure. The values of the above parameters were measured on one day before renal biopsy. Microscopic hematuria was defined as the presence of ≥25 red blood cells/mm^3. Nephrotic syndrome represented the presence of proteinuria of >50 mg/kg/24 h, with serum albumin level ≤25 g/L. Pure-tone audiometry and ophthalmological examination were carried out in 10 patients.

Assessment of renal histopathological changes

Percutaneous renal biopsy was performed in every patient during the initial evaluation.

Light microscopy: Renal tissue sections, 3 μm-thick, were stained with hematoxylin-eosin, periodic acid Schiff (PAS), Masson's trichrome, and silver methenamine for histopathological analysis. Tubulointerstitial chronic lesions, including tubular atrophy and interstitial fibrosis, and foam cell infiltration were scored semi-quantitatively using a scale of 0 to 3 as follows: 0. no obvious change; 1. lesions involving less than 25% of the area; 2. lesions affecting 25%-50%; 3. lesions involving more than 50%, according to the scoring system of Foster et al [12].

Immunofluorescence: Cryostat sections of frozen renal tissues were fixed in acetone and immunostained. For conventional examination, the renal specimen was stained directly by the fluorescein isothiocyanate (FITC)-conjugated anti-human IgA, IgG, IgM, C3, C4, Clq and fibrinogen antibodies. All antibodies were obtained from Dako (Glostrup, Denmark).

Immunofluorescence for localization of α3(IV) and α5(IV) chains in renal specimens was performed using monoclonal antibodies against α3(IV) and α5(IV) chains (Weislab, Lund, Sweden) in paraffin-embedded renal biopsies. First, 3 μm-thick sections were dewaxed in xylene and hydrated to distilled water through decreasing concentrations of alcohol, and subjected to heat-induced epitope retrieval with 0.01 M citrate buffer (pH 6.0) and pepsin digestion for 10 min. The primary antibody was diluted 1:50 in phosphate-buffered saline with 0.5% bovine serum albumin. Incubation was carried out for 60 min at 37°C, followed by 30 min incubation with 1:50 solution of FITC conjugated secondary antibody (Dako).

Electron microscopy: Renal specimens were available from 13 of the 16 cases for electron microscopy. The tissue specimen was fixed in

glutaraldehyde followed by osmium tetroxide and embedded in araldite. Ultrathin sections were examined generally after staining with the combination of lead citrate and uranyl acetate. The sections were independently examined and evaluated by two renal pathologists blinded to the clinical information.

Immunohistochemical analysis for AngII: AngII expression was detected in 16 renal biopsies from XLAS and 10 normal control renal tissues adjacent to carcinoma from surgical remove using immunohistochemistry. Staining for AngII was performed using formalin-fixed paraffin-embedded renal biopsies. Heat-induced epitope retrieval with 0.01 M citrate buffer (pH 6.0) was performed. Then slides were incubated with a rabbit polyclonal anti-AngII primary antibody (1:300, Bache, Torrance, CA) for 60 min at 37°C , followed by 30 min incubation with 1:50 solution of alkaline phosphatase (AP) conjugated secondary antibody (Zhongshan, Beijing, China). Immunodetection was performed using the Alkaline Phosphatase Enhanced Red kit (Zhongshan, Beijing, China). Nuclei were counterstained with hematoxylin. Ten normal renal tissues were used as control tissues samples. Ten constant fields in each biopsy tissue were acquired and the mean integral optical density (IOD) was calculated in a blind manner by two pathologists using image pro-plus software (Media Cybernetics, Rockville, MD).

Immunohistochemical analysis for other RAAS components: Sixteen renal biopsies from XLAS were stained using immunohistochemical method with anti-AGT antibody (Sigma Aldrich, rabbit polyclonal, 1:40 dilution), anti-renin antibody (Abcam, mouse polyclonal, 1:100 dilution), anti-ACE antibody (Sigma Aldrich, rabbit polyclonal, 1:100 dilution), anti-AT_1R antibody (Abcam, mouse monoclonal, 1:100 dilution). Staining were performed using formalin-fixed paraffin-embedded renal biopsies. Heat-induced epitope retrieval with 0.01 M citrate buffer (pH 6.0) was performed. Streptavidin-biotin complex immunodetection was performed using the DAB Detection System (Zhongshan, Beijing, China). Hematoxylin and PAS staining were performed to stain nuclei and basement membranes, respectively.

Genetic analysis

Genetic mutations of *COL4A3, COL4A4, COL4A5* were analyzed in three families using exon trapping-next generation sequencing technology, then verified the DNA sequence variant by sanger sequencing.

Statistical analysis

Data were presented as mean ± SD values. The relationship between expression of AngII and serum CysC level was assessed with the Pearson correlation. The relationships between AngII expression and tubulointerstitial chronic lesion and foam cell score were assessed with Spearman's rank correlation. Differences were considered significant when the *P* value was <0.05.

Results

Patients

The study subjects were 16 probands (12 boys and 4 girls) with XLAS. The mean age at renal biopsy was 9.5±4.8 years (range 3-17). The mean disease duration was 29.8±34.8 months (range 0.6-120).

Clinical features and family history

All 16 patients had microscopic hematuria, 8 (50%) patients presented with nephrotic syndrome (male 50%, female 50%), 1 case with nephrotic level proteinuria, 5 cases with hematuria and proteinuria, 2 cases had both persistent microscopic hematuria and intermittent attacks macroscopic hematuria, 1 patient had mildly low eGFR, 4 male patients with hypertension, 2 among 10 patients with high-tone sensorineural hearing loss, and 4 among 10 patients with ocular lesions . Analysis of family history showed 12 (75%) patients with family history of hematuria. Among them, 8 (50%) had family history of renal failure (**Table 1**).

Histopathological findings

Light microscopy: The mean number of glomeruli included in the renal biopsy specimens was 17.3±7.4 (range 8-29). Of 16 patients, 12 (75%) had fetal glomeruli and/or obliterated glomeruli, fetal glomeruli mean immature glomerular, 10 (62.5%) specimens showed various degrees of infiltration of foam cell. Among the 12 male patients, 5 (41.67%) had focal segmental glomerular sclerosis, 11 (91.67%) had minor-to-moderate chronic tubulointerstitial lesions (**Table 2**).

Immunofluorescence and genetic analysis

The expression levels of α5(IV) and α3(IV) chains were analyzed in all renal specimens.

Table 1. Clinical features of the 16 children with XLAS

Case no	Age (yrs)	Sex	Duration (months)	Family history (Y/N)	Hematuria mac (Y/N) mic (RBC/m^3)	Clinical presentation	CysC (mg/l)	Ccr (ml/min/ 1.73 m^2)	Hearing defect	Ocular defect	SBP/DBP (mmHg)
1	3	M	3	Y	Y (3394)	Hematuria and proteinuria	0.86	108.8	-	-	86/54
2	4	M	11	Y	N (290.6)	Nephrotic syndrome	0.85	102.9	Normal	Normal	118/72
3	5	M	32	Y	Y (666.1)	Hematuria and proteinuria	1.11	101.4	-	-	84/56
4	7	M	4	Y (RF)	N (381.2)	Nephrotic syndrome	0.91	115.5	Normal	Abnormal	90/60
5	8	M	6	Y (RF)	N (329)	Nephrotic syndrome	1.12	108.0	Normal	Normal	98/60
6	11	M	72	Y (RF)	N (728)	Nephrotic syndrome	0.72	119.2	Abnormal	Normal	138/100
7	12	M	18	N	N (92)	Nephrotic level proteinuria	1.17	101	Normal	Abnormal	100/70
8	13	M	6	Y (RF)	N (750.6)	Nephrotic syndrome	0.85	111.2	-	-	120/88
9	15	M	2	Y (RF)	N (225.4)	Hematuria and proteinuria	0.88	96.2	-	-	120/80
10	16	M	39	N	N (219)	Nephrotic syndrome	1.00	104.6	Normal	Abnormal	110/60
11	17	M	12	Y	N (143.9)	Hematuria and proteinuria	1.90	91.4	Normal	Abnormal	159/106
12	17	M	120	Y (RF)	N (79.4)	Hematuria and proteinuria	2.59	84.2	Abnormal	Normal	164/108
13	5	F	1	N	N (200)	Isolated hematuria	0.90	112.8	-	-	90/60
14	8	F	48	Y (RF)	N (604)	Nephrotic syndrome	0.79	157.2	Normal	Normal	95/70
15	9	F	84	N	N (264)	Nephrotic syndrome	0.93	98.4	-	-	85/60
16	12	F	60	Y (RF)	N (150.5)	Isolated hematuria	0.84	109.4	Normal	Normal	90/70

Abbreviations: M: male; F: female; Mac: macrohematuria; Mic: microhematuria; RF: renal failure; CysC: cystatin C; Ccr: creatinine clearance; -: not identified.

Table 2. Pathological features of the 16 children with XLAS

Case no	Light microscopy				Electron microscopy				Expression of collagen IV					
	No of glomeruli	OG (%)	SS (%)	CTI lesion	IFC	GBM		EFP	GBM		BM		TBM	
						Thick	Split		Col4α3	Col4α5	Col4α3	Col4α5	Col4α3	Col4α5
1	20	15	0	1	0	+	+	Segment	-	-	-	-	-	-
2	27	0	0	0	0	+	+	Diffuse	-	-	-	-	-	-
3	14	28.57	0	1	0	+	+	Segment	-	-	-	-	-	-
4	29	6.90	0	1	2	+	+	Diffuse	-	-	-	-	-	-
5	18	5.56	0	1	1				-	-	-	-	-	-
6	17	17.65	5.88	1	2				-	-	-	-	-	-
7	15	13.33	13.33	1	1	+	+	Diffuse	-	-	-	-	-	-
8	10	0	10	1	2				-	-	-	-	-	-
9	9	22.2	0	1	2	+	+	Diffuse	-	-	-	+	-	-
10	16	18.75	0	1	2	+	+	Diffuse	-	-	-	-	-	-
11	8	12.5	25	2	2	+	+	Diffuse	-	-	-	-	-	-
12	17	23.53	5.88	1	2	+	+	Diffuse	-	-	-	+	-	-
13	14	7.14	0	0	0	+	+	Segment	Seg+	Seg+	-	Seg+	Seg+	Seg+
14	28	3.57	0	0	0	+	+	Diffuse	Seg+	Seg+	-	Seg+	Seg+	Seg+
15	8	0	0	0	1	+	+	Segment	Seg+	Seg+	-	Seg+	Seg+	Seg+
16	16	0	0	1	0	+	+	Segment	Seg+	Seg+	-	Seg+	Seg+	Seg+

Abbreviations: OG: obliterate glomeruli; SS: segmental sclerosis; CTI: chronic tubulointerstitial; IFC: interstitial foam cells; GBM: glomerular basement membrane; split: splitting; EFP: effacement of foot process; BM: Bowman's membrane; TBM: tubular basement membrane; +: positive expression; -: negative expression.

All four female patients presented α5(IV) and α3(IV) segmental expression in GBM and tubular basement membrane (**Table 2**), the representative staining of α5(IV) was showed in patient 14 (**Figure 1A**). Patient 14, an 8-year-old girl with 4-year history of nephrotic syndrome and family history of renal failure, underwent genetic testing. A nonsense mutation of Arg373Ter was found in 19 exon of *COL4A5*. The mutation was associated with early termination of amino-acid coding, which was considered to potentially affect protein function. The same mutation type and locus were verified in the relatives (mother and grandmothers had

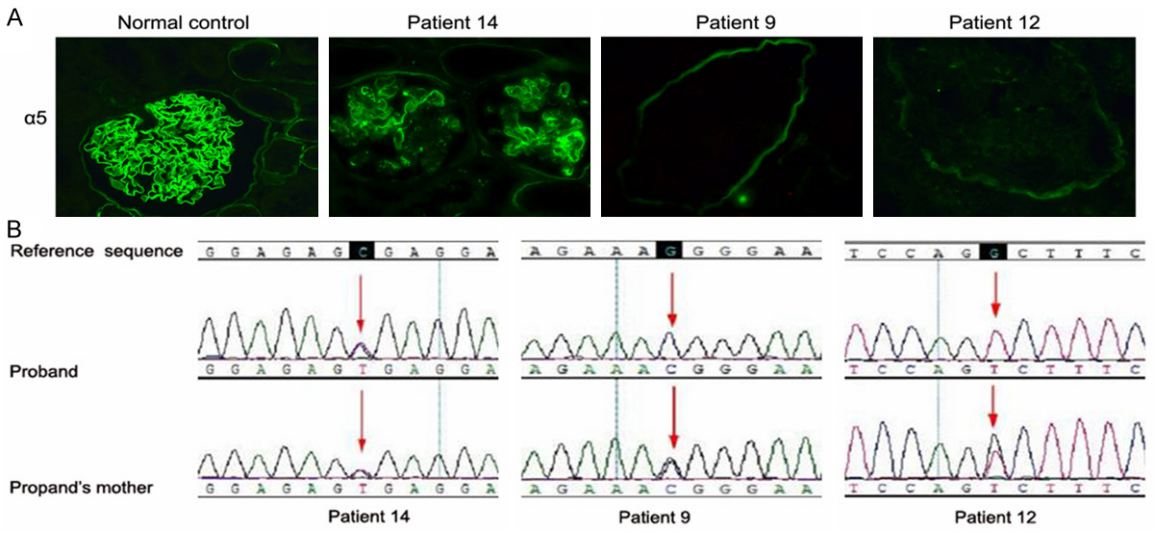

Figure 1. Immunofluorescence for localization of α5(IV) chain in renal specimens and gene mutation analysis. A. Expression of α5(IV) chain in normal renal section and in typical female and atypical male patients with XLAS. Linear expression was seen in normal GBM, Bowman's capsule and tubular basement membrane, segmental deletion in patient 14, and weakly positive expression in Bowman's capsule in patient 9 and patient 12. Magnification: × 400. B. Three pathogenic mutations of *COL4A5* gene in patient 14, 9 and 12. Patient 14 had a heterozygous C→T mutation at 1117 bp of the coding region with amino acid substitution of Arg for Ter at codon 19. The mother had identical heterozygous mutation. Arrows point to the mutation position. Patient 9 had a hemizygous G→C mutation at 1543 bp of the coding region with amino acid substitution of Gly for Arg at codon 23. The mother of this patient had identical heterozygous mutation. Arrows point to the mutation position. Patient 12 had a hemizygous G→T mutation at 1616 bp of coding region with amino acid substitution of Gly for Val at codon 24. The mother had identical heterozygous mutation. Arrows point to the mutation position.

the same heterozygous mutation, and the younger brother had hemizygous mutation in the same locus) by pedigree validation.

Among the 12 male patients, 10 showed negative expression of α5(IV) and α3(IV) in GBM, Bowman's capsule and tubular basement membrane, but patient 9 and patient 12 showed weakly expression of α5(IV) in Bowman's capsule only (**Table 2**, **Figure 1A**). Therefore, autosomal dominant hereditary of AS was not be excepted according to the expression pattern of α5(IV) chain in two patients. To determine the diagnosis, the exons of the *COL4A3, COL4A4, COL4A5* gene were screened for mutations by using NGS. Our results showed that both of them were actually X-linked dominant hereditary by genetic analysis and pedigree validation (**Figure 1B**), One with Gly515Arg in 23 exon of *COL4A5*, and the other with Gly539Val in 24 exon of *COL4A5*.

Electron microscopy: All 13 specimens showed variable degree of irregular attenuation and thickening of the GBM, along with splitting of lamina densa and effacement of podocyte foot process. 8 cases showed diffuse effacement of podocyte foot process, and 5 showed segmental effacement of podocyte foot process (**Table 2**).

Renal expression of angiotensin II and other RAAS components

In normal control renal tissues, AngII was weakly expressed in lumen border of some distal tubular cells (**Figure 2A**). However, AngII expression was enhanced in the cytoplasm of tubular epithelial cells (**Figure 2B**), lumen border of the tubules (**Figure 2C**), interstitium (**Figure 2C**) and foam cells (**Figure 2D**) in renal tissues of XLAS. The intensity of immunoreactivity for AngII showed significantly higher in renal tissues of XLAS (4740±680 arbitrary unit) than that of normal control (291±42 arbitrary unit).

In normal renal tissues, AGT was weakly expressed as granular pattern in the cytoplasm of tubular epithelial cells. Renin was expressed in the cytoplasm or apical membranes of few tubular epithelial cells and in juxtaglomerular apparatus. ACE was detected in lumen border of some tubular epithelial cells and smaller

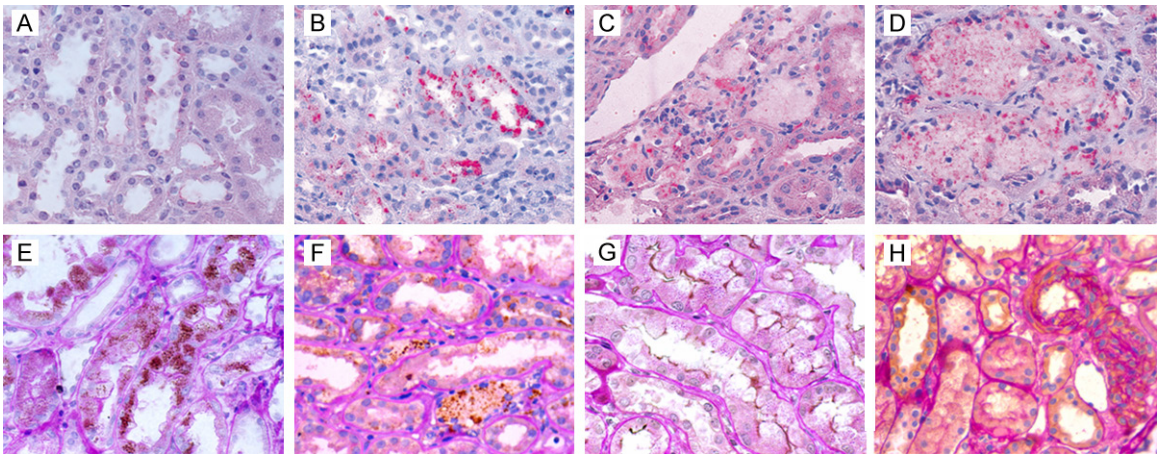

Figure 2. Immunohistochemical analysis of AngII and other RAAS components in renal tissues of XLAS. A. Expression of AngII in the lumen border of tubular cells in normal control. B. Expression of AngII in the cytoplasm of tubular epithelial cells in XLAS. C. Expression of AngII in the lumen border of tubular cells and interstitium in XLAS. D. Expression of AngII in foam cells in XLAS. E. Expression of AGT in the cytoplasm of tubular epithelial cells. F. Expression of the renin in the cytoplasm of tubular epithelial cells and interstitial foam cells. G. Expression of ACE in lumen border of the tubules. H. Expression of AT_1R in membrane and cytoplasm of some tubular epithelial cells. Original magnifications: A-D. Immunohistochemistry with hematoxylin counterstain; E-H. Immunohistochemistry with PAS counterstain; all × 400.

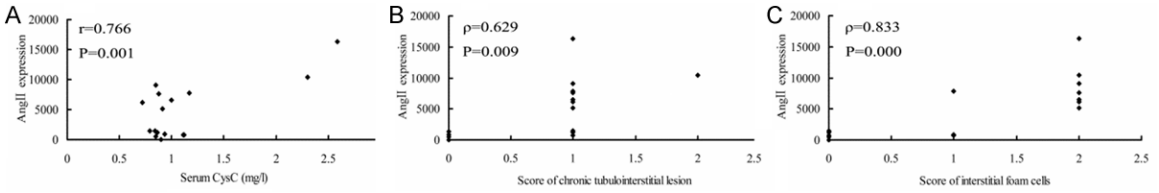

Figure 3. Correlations between renal expression of AngII and CysC , score of chronic tubulointerstitial lesion, and foam cell score. A. Correlations between renal expression of AngII and CysC. B. Correlations between renal expression of AngII and score of chronic tubulointerstitial lesion. C. Correlations between renal expression of AngII and foam cell score.

arteries, and AT_1R was found in membrane and cytoplasm of some tubular epithelial cells and smaller arteries. In XLAS patients' renal tissues, AGT expression was enhanced in the cytoplasm of some tubular epithelial cells (**Figure 2E**), and renin expression was also obviously increased in the cytoplasm of some tubular epithelial cells and interstitial foam cells (**Figure 2F**) in XLAS. No obvious changes of ACE (**Figure 2G**) and AT_1R (**Figure 2H**) expression was seen in XLAS.

Serum CysC level correlated with renal AngII immunostaining intensity (r=0.766, P=0.001, **Figure 3A**). Chronic tubulointerstitial lesions and foam cell scores also correlated with renal AngII immunostaining intensity (ρ=0.629, P=0.009 and ρ=0.833, P=0.000, respectively, **Figure 3B**, **3C**).

Discussion

The present study demonstrated that proteinuria and nephrotic syndrome are not unusual in pediatric XLAS, and that clinical manifestations can also be seen in female patients. It is generally thought that the affected females in XLAS kindred typically display mild clinical involvement, particularly during childhood and young adulthood [13]. In our study, proteinuria was noted in all 12 male patients and in 2 of 4 female patients, while nephrotic syndrome developed in 6 of 12 (50%) male patients and 2 of 4 (50%) female patients. These rates are higher than those reported in previous studies in China [14]. The high rates in our study might be related to inclusion of inpatient only and/or the small sample size. Grünfeld et al [15] found that history of gross hematuria in childhood

and presence of nephrotic syndrome were significant predictors of poor prognosis in female XLAS patients. Therefore, the female XLAS patients with serious clinical manifestations in our study should be followed up closely in the future.

Before the use of electron microscopy, AS was considered as tubulointerstitial nephritis and the only diagnostic feature was the detection of interstitial foam cells. In our study, 11 (92%) male patients had minor-to-moderate chronic tubulointerstitial lesions, and 9 (75%) cases had variable degree of foam cell infiltration. Among the 4 female patients, 1 (25%) showed interstitial infiltration of foam cell. Our data also showed that chronic tubulointerstitial lesions and foam cell infiltration were not parallel with obvious glomerular lesions and clinical presentation completely. Focal areas of interstitial fibrosis was seen before the appearance of obvious glomerular lesions, as reported by Noël [16]. Since XLAS is a classic model for basement membrane lesion, including glomerular and tubular basement membranes, renal tubular lesion may exist independent of glomerular lesion. On the other hand, the loss of effective GBM barrier allows ultrafiltered albumin and other plasma proteins access to the proximal tubular lumen, which triggers various proinflammatory and profibrotic signaling pathways in proximal tubular epithelial cells [17, 18]. Therefore, proteinuria leading to tubulointerstitial injury is multifactorial and its pathogenic role cannot be ignored in XLAS.

ACEI as the first-line agents for AS treatment [9]. ACEI prolong renal survival and delay the need for renal transplantation by reducing circulating AngII levels and blood flow pressure [19]. AngII is produced both in the circulation and local renal tissue [20, 21]. Our results showed the enhanced intrarenal AngII expression in the tubules, interstitium and foam cells of XLAS, and the expression correlated with local tubulointerstitial pathology. These results suggest that intrarenal AngII plays an important role in disease progression. What is the possible mechanism of intrarenal AngII overexpression in XLAS? First, tubular epithelial cells resorb AngII from glomerular filtration via the AT_1R [21, 22]. Second, in the kidney, all the components needed for AngII synthesis are present within the renal interstitium, tubular epithelial cells and luminal fluid [23]. Similarly, AGT, renin, ACE and AT_1R were expressed in tubular epithelial cells and renin also was seen in interstitium and foam cells in our study. AGT is the only known substrate for renin [24], and progressive injury of the GBM filtration barrier in XLAS allows more circulating AGT into tubular fluid, and provides abundant substrate for intratubular and interstitial synthesis of AngI and AngII. Third, macrophages express all components of the renin-angiotensin system and release AngII [25].

On the other hand, interstitial AngII can also be resorbed into macrophages. Rafatian et al [26] demonstrated that AngII can induce transformation of macrophages into foam cells *in vitro*. Other groups showed that AngII overexpression enhances foam cell formation in atherosclerosis [27, 28]. Our data suggest that the intrarenal AngII upregulation is probably the major stimulus of foam cell formation in XLAS. Therefore, intrarenal activation of AngII not only promote foam cell formation but also aggravate chronic injury of the tubulointerstitium in XLAS.

In present study, two new glycine replacement missense mutations were identified. One is Gly515Arg in exon 23 of *COL4A5*, and the other is Gly539Val in exon 24 of *COL4A5*. Both mutations were considered deleterious. Gross et al [29] proposed the following classification of phenotypes of XLAS: (a) Severe type, characterized by juvenile-onset ESRD (~20 years of age), caused by extensive rearrangements, premature stop, frameshift, donor splice site, and mutations in the NC1-domain. (b) Moderate-Severe type, including patients that progress to ESRD (~26 years of age), with non-glycine missense mutations, glycine substitutions in exons 21-47, in-frame and acceptor splice site mutations. (c) Moderate type, associated with glycine substitutions in exons 1-20 and characterized by late-onset ESRD (~30 years of age). It is reasonable to conclude that the two new glycine missense mutations identified in our study belong to the Moderate-Severe type and two pedigrees had family history of renal failure. One nonsense mutation of Arg373Ter reported by Renieri [30], was detected in exon 19 of *COL4A5* in a single 8-year-old girl with 4-year history of NS, who had a family history of renal failure. Based on Gross et al [29] classification,

her nonsense mutation could be classified as XLAS severe type.

Therefore, the *COL4A5* mutation type, persistent proteinuria, and the enhanced intrarenal AngII were all responsible for the progression of XLAS. Furthermore, the intrarenal AngII overexpression may play an important role in tubulointerstitial lesions and foam cell formation.

Acknowledgements

This work was partly supported by Talents support fund for science and technology innovation in colleges and universities of Henan province (No. 2012HASTIT019) and Henan science and technology innovation talents program (outstanding youth) in 2014 (No. 144100510014).

Disclosure of conflict of interest

None.

Address correspondence to: Yanjie Huang, Department of Pediatrics, The First Affiliated Hospital of Henan University of Traditional Chinese Medicine, 19 Renmin Road, Henan 450000, China. Tel: +86-371-66264832; Fax: +86-371-65990568; E-mail: huangyanjie69@hotmail.com; huangyanjie69@163.com

References

[1] Kashtan CE. Alport syndromes: phenotypic heterogeneity of progressive hereditary nephritis. Pediatr Nephrol 2000; 14: 502-512.

[2] Yoshikawa N, Ito H, Matsuyama S, Hazikano H, Okada S, Matsuo T. Hereditary nephritis in children with and without characteristic glomerular basement membrane alterations. Clin Nephrol 1988; 30: 122-127.

[3] Hostikka SL, Eddy RL, Byers MG, Hoyhtya M, Shows TB, Tryggvason K. Identification of a distinct type IV collagen alpha chain with restricted kidney distribution and assignment of its gene to the locus of X chromosome-linked Alport syndrome. Proc Natl Acad Sci U S A 1990; 87: 1606-1610.

[4] Coppo R, Gianoglio B, Porcellini MG, Maringhini S. Frequency of renal diseases and clinical indications for renal biopsy in children (report of the Italian National Registry of Renal Biopsies in Children). Group of Renal Immunopathology of the Italian Society of Pediatric Nephrology and Group of Renal Immunopathology of the Italian Society of Nephrology. Nephrol Dial Transplant 1998; 13: 293-297.

[5] Li LS, Liu ZH. Epidemiologic data of renal diseases from a single unit in China: analysis based on 13,519 renal biopsies. Kidney Int 2004; 66: 920-923.

[6] Hudson BG, Tryggvason K, Sundaramoorthy M, Neilson EG. Alport's syndrome, Goodpasture's syndrome, and type IV collagen. N Engl J Med 2003; 348: 2543-2556.

[7] Jais JP, Knebelmann B, Giatras I, De Marchi M, Rizzoni G, Renieri A, Weber M, Gross O, Netzer KO, Flinter F, Pirson Y, Dahan K, Wieslander J, Persson U, Tryggvason K, Martin P, Hertz JM, Schröder C, Sanak M, Carvalho MF, Saus J, Antignac C, Smeets H, Gubler MC. X-linked Alport syndrome: natural history and genotype-phenotype correlations in girls and women belonging to 195 families: a "European Community Alport Syndrome Concerted Action" study. J Am Soc Nephrol 2003; 14: 2603-2610.

[8] Jais JP, Knebelmann B, Giatras I, De Marchi M, Rizzoni G, Renieri A, Weber M, Gross O, Netzer KO, Flinter F, Pirson Y, Verellen C, Wieslander J, Persson U, Tryggvason K, Martin P, Hertz JM, Schröder C, Sanak M, Krejcova S, Carvalho MF, Saus J, Antignac C, Smeets H, Gubler MC. X-linked Alport syndrome: natural history in 195 families and genotype- phenotype correlations in males. J Am Soc Nephrol 2000; 11: 649-657.

[9] Kashtan CE, Ding J, Gregory M, Gross O, Heidet L, Knebelmann B, Rheault M, Licht C. Clinical practice recommendations for the treatment of Alport syndrome: a statement of the Alport Syndrome Research Collaborative. Pediatr Nephrol 2013; 28: 5-11.

[10] Yamamoto T, Nakagawa T, Suzuki H, Ohashi N, Fukasawa H, Fujigaki Y, Kato A, Nakamura Y, Suzuki F, Hishida A. Urinary angiotensinogen as a marker of intrarenal angiotensin II activity associated with deterioration of renal function in patients with chronic kidney disease. J Am Soc Nephrol 2007; 18: 1558-1565.

[11] Flinter FA, Cameron JS, Chantler C, Houston I, Bobrow M. Genetics of classic Alport's syndrome. Lancet 1988; 2: 1005-1007.

[12] Foster BJ, Bernard C, Drummond KN, Sharma AK. Effective therapy for severe Henoch-Schonlein purpura nephritis with prednisone and azathioprine: a clinical and histopathologic study. J Pediatr 2000; 136: 370-375.

[13] Rheault MN. Women and Alport syndrome. Pediatr Nephrol 2012; 27: 41-46.

[14] Wang F, Ding J, Guo S, Yang J. Phenotypic and genotypic features of Alport syndrome in Chinese children. Pediatr Nephrol 2002; 17: 1013-1020.

[15] Grunfeld JP, Noel LH, Hafez S, Droz D. Renal prognosis in women with hereditary nephritis. Clin Nephrol 1985; 23: 267-271.

[16] Noel LH. Renal pathology and ultrastructural findings in Alport's syndrome. Ren Fail 2000; 22: 751-758.
[17] Abbate M, Zoja C, Remuzzi G. How does proteinuria cause progressive renal damage? J Am Soc Nephrol 2006; 17: 2974-2984.
[18] Baines RJ, Brunskill NJ. Tubular toxicity of proteinuria. Nat Rev Nephrol 2011; 7: 177-180.
[19] Noone D, Licht C. An update on the pathomechanisms and future therapies of Alport syndrome. Pediatr Nephrol 2013; 28: 1025-1036.
[20] Wilcox CS, Peart WS. Release of renin and angiotensin II into plasma and lymph during hyperchloremia. Am J Physiol 1987; 253: F734-741.
[21] Zou LX, Imig JD, von Thun AM, Hymel A, Ono H, Navar LG. Receptor-mediated intrarenal angiotensin II augmentation in angiotensin II-infused rats. Hypertension 1996; 28: 669-677.
[22] Zou LX, Hymel A, Imig JD, Navar LG. Renal accumulation of circulating angiotensin II in angiotensin II-infused rats. Hypertension 1996; 27: 658-662.
[23] Navar LG, Harrison-Bernard LM, Nishiyama A, Kobori H. Regulation of intrarenal angiotensin II in hypertension. Hypertension 2002; 39: 316-322.
[24] Gould AB, Green D. Kinetics of the human renin and human substrate reaction. Cardiovasc Res 1971; 5: 86-89.
[25] Okamura A, Rakugi H, Ohishi M, Yanagitani Y, Takiuchi S, Moriguchi K, Fennessy PA, Higaki J, Ogihara T. Upregulation of renin-angiotensin system during differentiation of monocytes to macrophages. J Hypertens 1999; 17: 537-545.
[26] Rafatian N, Milne RW, Leenen FH, Whitman SC. Role of renin-angiotensin system in activation of macrophages by modified lipoproteins. Am J Physiol Heart Circ Physiol 2013; 305: H1309-1320.
[27] Leenen FH, White R, Yuan B. Isoproterenol-induced cardiac hypertrophy: role of circulatory versus cardiac renin-angiotensin system. Am J Physiol Heart Circ Physiol 2001; 281: H2410-2416.
[28] Zhao X, White R, Van Huysse J, Leenen FH. Cardiac hypertrophy and cardiac renin-angiotensin system in Dahl rats on high salt intake. J Hypertens 2000; 18: 1319-1326.
[29] Gross O, Netzer KO, Lambrecht R, Seibold S, Weber M. Meta-analysis of genotype-phenotype correlation in X-linked Alport syndrome: impact on clinical counselling. Nephrol Dial Transplant 2002; 17: 1218-1227.
[30] Renieri A, Bruttini M, Galli L, Zanelli P, Neri T, Rossetti S, Turco A, Heiskari N, Zhou J, Gusmano R, Massella L, Banfi G, Scolari F, Sessa A, Rizzoni G, Tryggvason K, Pignatti PF, Savi M, Ballabio A, De Marchi M. X-linked Alport syndrome: an SSCP-based mutation survey over all 51 exons of the COL4A5 gene. Am J Hum Genet 1996; 58: 1192-1204.